Egypt. J. Soil Sci. **Vol. 63**, No. 4, pp: 537-552 (2023)

Egyptian Journal of Soil Science

http://ejss.journals.ekb.eg/

Graphene Oxide Synthesis and Characterizations as a Carbonaceous Nanoparticle by Using Modified Hummers' Method

Marwa I. Ibrahim[a,b], Elsayed A. Awad[b], Salah M. Dahdouh[b] and **Wafaa M. El-Etr[a]***

[a] *Department of Soil Physics and Chemistry, Soil, Water and Environment Research Institute (SWERI), Agricultural Research Center (ARC), Egypt*
[b] *Department of Soil Science, Faculty of Agriculture, Zagazig University, Egypt*

THE SCIENTIFIC community has been more interested in nanomaterials based on graphene because of their distinctive chemical and physical characteristics. Recently, agricultural fields have routinely employed graphene oxide (GO). This study aims to produce graphene oxide using a modified Hummers method without sodium nitrate, using an environmentally friendly approach. The process involves the chemical oxidation of commercial graphite powder into graphene oxide using the modified Hummer's method. Also, the current study included the characterization of graphene oxide (GO) by X-ray diffraction (XRD), ultraviolet-visible spectrometer (UV-vis), scanning electron microscopy (SEM), transmission electron microscopy (TEM), Fourier transform infrared (FT-IR), atomic force microscopy (AFM), and elemental analysis (EA) were all used in the GO characterization. GO was evaluated using TEM images, which revealed that the GO sheets exhibited single and double lamellar layer structures with irregular forms and a thickness of 23 nm. The XRD patterns indicated that the GO peak centered at 2θ value 24º corresponds to an interplanar distance of carbon atoms arranged in (002) hexagonal layers; the interlayer spacing is approximately 8.61 Å according to the Scherrer equation. The oxygen-containing functional groups' presence in GO films like hydroxyl, carboxyl, epoxy, carbonyl, and C=C bunches was explained by a Fourier-change infrared spectrum analyzer (FT-IR) due to graphite oxidization in GO without twisting in the graphite layer structure. According to EA findings, the GO sheet's C element content was approximately 47.15 percent, O was 51.8%, H was less than 0.01%, and N was 1.02%. The UV-VIS spectrometer study revealed that the GO sheet exhibited an excellent optical reaction. The thickness and sidelong shape study of graphene oxide sheets by using atomic force microscopy (AFM). The SEM micrographs of GO obtained using modified Hummers handling demonstrate that the GO is made of two-dimensional sheets.

Keywords: Graphite; graphene oxide; modified Hummers' method; structure characteristic.

1. Introduction

The agricultural sector is critical for delivering food, feed, fiber, and fuel, but it suffers from a variety of losses due to abiotic stress, pathogen infestation, and soil fertility reduction (Badgar et al., 2021). Nanotechnology has the ability to increase the efficiency and quality of agricultural output while potentially addressing prevalent issues (El-Shahawy et al., 2022). Nanomaterials (NMs) have been found to promote soil stability and sequestration due to their unique properties (Ghazi et al., 2022). Also, NMs have the ability to form and interact with organic colloids, making them effective in C sequestration (Pramanik et al., 2020). However, Kumar and Jalageri (2020) reported that carbon-derived nanomaterials like graphene and its derivatives (GO, rGO), carbon nanotubes, and activated carbons have a unique structure. These materials have an absorption capacity, electrical and electronic properties, and acidity. It has developed an

*Corresponding author e-mail: merofad2008@gmail.com
Received: 28/07/2023; Accepted: 04/09/2023
DOI: 10.21608/EJSS.2023.225259.1624

interest in nanomaterials for various applications like physics, chemistry, biology, and medicine (Seyed and Shabnam, 2017). Also, they play an important role as adsorbents in soil, controlling OM fixation, regulating nutrient transport, and promoting the precipitation of new mineral phases (Mani and Mondal, 2016). Future research will depend heavily on in situ, undamaged soil structures.

Graphene has demonstrated potential as a material for photoelectronic, biological, and sensing applications among all of these carbon-based nanomaterials (Eigler and Hirsch, 2014). Graphene is a two-dimensional honeycomb structural material comprised of a single atomic layer of carbon atoms arranged in a hexagonal lattice, according to Wang and Shi (2015). Additionally, according to Huang et al. (2011), graphene has extraordinary properties, such as a large surface area of 2630 m_2g^{-1}, Young's modulus of 1.0 TPa, and a 130 GPa tensile strength. According to Dreyer et al. (2010), GO has demonstrated exceptional dependability in a number of applications, which may be attributed to its unique physicochemical properties such as its large surface area and mechanical soundness. These physicochemical features have created new agricultural options, such as slow-release fertilizers. Also, Pendolino and Armata (2017); Smith et al. (2019) and Zaaba et al. (2017) detailed that, chemically, graphene sheets have been combined with oxygen functional groups like hydroxyl (OH), alkoxy (COC), carbonyl (CO), carboxylic acid (COOH), and other oxygen-based groups in graphene oxide (GO), an oxidized form of graphene. These oxygenated bunches are liable for numerous benefits over graphene, including higher dissolvability.

Hummers and Offeman (Hummers and Offeman, 1958), who produced graphite oxide through the graphite oxidation process using different techniques, are commonly given credit for creating graphene oxide. Both processes were improved by Hummers and Offeman in a number of ways to make them safer, including the use of sodium nitrate and the addition of the oxidant $KMnO_4$. The Hummers approach is mostly used to produce GO because of its higher level of security and adaptability. Another modification, known as "the further developed Hummers" technique, replaced sodium nitrite with phosphoric acid expansion and increased the quantity of $KMnO_4$. This method yields GO powders with a greater level of oxidation while producing no harmful gases and only a little degree of temperature control. According to Marcano et al. (2010), this "further developed hummers" approach has advantages such as carbon material that is more hydrophilic and has similar conductivity and no harmful gases are released in the process. Moreover, Shin et al. (2013) found that the Hummers method's blend of sulfuric acid and nitric acid functions as a "chemical scissors" for graphene planes, allowing the oxidation solution to penetrate potassium permanganate which, on the other hand, may accomplish full intercalation of graphite, resulting in graphite bisulfate (Avdeev et al., 1992; Sorokina et al., 2005). This interaction guarantees that potassium permanganate may effectively penetrate the graphene layers for graphite oxidation. As a result, potassium permanganate takes over the role of sodium nitrate. So, this method provides a simple synthesis pathway for producing GO utilizing a low-cost and ecologically friendly modified Hummers technique. Recently, Méndez-Lozano et al. (2022) added that the technique for GO synthesis created by Hummers and Offeman (1958) is the most significant and often used. Over other methods, this one offers three key advantages. First, the reaction is finished in a short period of time; second, potassium permanganate can be used in place of potassium chlorate for a safer reaction; and third, using sodium nitrate prevents the development of acid mist. The approach does, however, have some flaws, as the oxidation process releases several harmful gases, such as nitrogen dioxide and dinitrogen tetroxide. Additionally, it is challenging to remove salt and nitrate ions from the wastewater produced during the production and purification of graphene oxide.

Moreover, Singh et al. (2016) added that graphite powder is converted into graphene oxide, an oxidized version of graphene, using a chemical oxidation process. For the production of graphene oxide, a number of processes have been reported, including chemical vapor deposition, mechanical exfoliation, and high-vacuum annealing. None of these methods are preferred and are not presently being used due to their disadvantages, which include their toxicity, cost, and time requirements (Song et al., 2014 and Singh et al., 2018). Chemical methods are considered to be the most promising means of producing graphene oxide in order to overcome all of its disadvantages (cost, time, and toxicity) because of its excellent water solubility (Xing et al., 2016). According to Kiang Chua and Pumera (2014) and Wang et al. (2013), techniques for producing graphene may be roughly split into two categories: those that employ simple carbon particles and those that entail peeling layers of derivatives of graphene from a carbon source, frequently graphite. The first synthesis category is time-consuming and has scalability concerns, claim Wang et al. (2018). The second classification approach, which is better recognized for detecting graphene derivatives and was responsible for the creation of GO, particularly for usage in nanocomposite materials, is now in the spotlight. On the other hand, Song et al. (2014) and Abaszade et al. (2021) mentioned that GO sheets could be characterized by many various analytical

techniques such as Fourier transform infrared spectroscopy (FTIR), Electron microscopic techniques (Scanning electron microscopy (SEM) and Transmission electron microscopy (TEM), powder X-ray diffraction analysis (XRD) and UV-Vis spectroscopy (UV-VIS).

In the present research, the straight-forward, rapid, and affordable modified hummers technique have been used to generate GO. Additionally, this process creates hydrophilic groups inside the carbon material, which reduces the creation of harmful gases and improves conductivity. With the goal of producing pure graphene oxide for upcoming applications and the resulting graphene oxide has been analyzed.

2. Materials and methods

International Chemicals Company provided 99.5% pure graphite material (natural, 150 mesh) for the production of GO nanoparticles.

1. Graphene oxide preparation by a modified Hummers' method

Pure graphite powder was utilized in the conventional approach, the modified Hummers' method described by Zaaba et al. (2017), to create graphene oxide (GO). For many minutes, combine and stir 27 ml of sulfuric acid (H_2SO_4) and 3 ml of phosphoric acid (H_3PO_4) at a 9:1 volume ratio. After that, 0.225 g of graphite powder was placed in the mixing fluid and forcefully mixed potassium permanganate ($KMnO_4$) was then gradually added to the mixture in a 1.32 g amount. A light green mixture was produced after six hours of mixing this concoction. In order to remove the excess $KMnO_4$, 0.675 ml of hydrogen peroxide (H_2O_2) was progressively added and agitated for 10 minutes. It cooled as a result of an exothermic process. The resulting mixture was centrifuged for 7 minutes at 5,000 rpm after adding 30 ml of deionized water and 10 ml of HCl. The supernatant was then decanted away and the residue was washed several times with HCl and DIW. Then the cleaned GO solution was dried for 24 h in a 90 °C oven to create the GO powder.

2. Characterization of graphene oxide

1. GO sheet's minuscule morphologies were described by transmission electron microscopy (TEM; JEOL Inc., JEM1010) **(Bystrzejewski et al., 2007; Morishige and Hamada, 2005)**. To set up the example for TEM imaging, a drop of GO suspension was put on a nickel lattice and allowed to evaporate.
2. As described by **Dubin et al. (2010) and Li et al. (2011),** the spaces between the interlayers of GO sheets, which specified the graphene oxide exfoliation degree, were discovered by X-ray diffraction (XRD; Rigaku Inc., Ultima IV).
3. The Fourier-transform infrared spectra analyzer (Backman-IR 250 double beam grading spectrophotometer) was used to measure the structures of the GO sheets. The scanning range was 400 to 4000 cm^{-1}. At the Micro Analytical Centre, Cairo University, the dried powder was prepared for infrared spectra using the KBr pellets technique described by **Stankovich et al. (2007).**
4. The elemental composition of GO sheets was analyzed by an Antomatic analyzer CHNS (Varioel 111 elementer) at Microanalytically Center, Cairo University. Oxygen was determined by deducting the aggregate sum of carbon%, nitrogen %, hydrogen % and sulfur % from 100 **(Zhao et al. 2015).**
5. UV spectrometer (UV-VIS; Unicam UV300, Thermo Spectronic, USA) was utilized to test the GO sheet's optical absorption characteristics in order to confirm the existence of the sample's characteristic C=O and C=C chromophores.
6. Atomic force microscopy (AFM) analysis was carried out using a Shimadzu (SPM 9600) Japan scanner.
7. Quanta's FEG 250 scanning electron microscope (SEM) was used to examine the sample's morphologies at magnifications of 1000 X, 5000 X, and 10000X with an accelerating voltage of 20 kV.

3. Results

At first, the modified Hummers' method was used in the production process of graphene oxide by oxidation of purified natural flake graphite (NFG). Then, using an ultrasonic instrument, graphite oxide was exfoliated in distilled water to create graphene oxide (GO).

Graphene oxide properties

Graphene oxide is made up of carbon atoms bonded in single or very thin layers to various groups such as carbonyl, hydroxyl, carboxyl, and epoxy. There is considerable dispute over the precise structure of graphene oxide. The method of synthesis determines the kind, quantity, and distribution of various groups present in graphene oxide, whereas the method and features of the reducing agent determine the reduction.

The GO characterization

1. Transmission electron microscopy (TEM)

The properties of the GO film were thoroughly characterized. The TEM image analysis (Fig. 1) revealed that the produced GO sheets had a single and two-fold laminar layer structure with a 23 nm thickness. Kabiri et al. (2017) employed a TEM picture of GO to confirm their optimum size and uneven form.

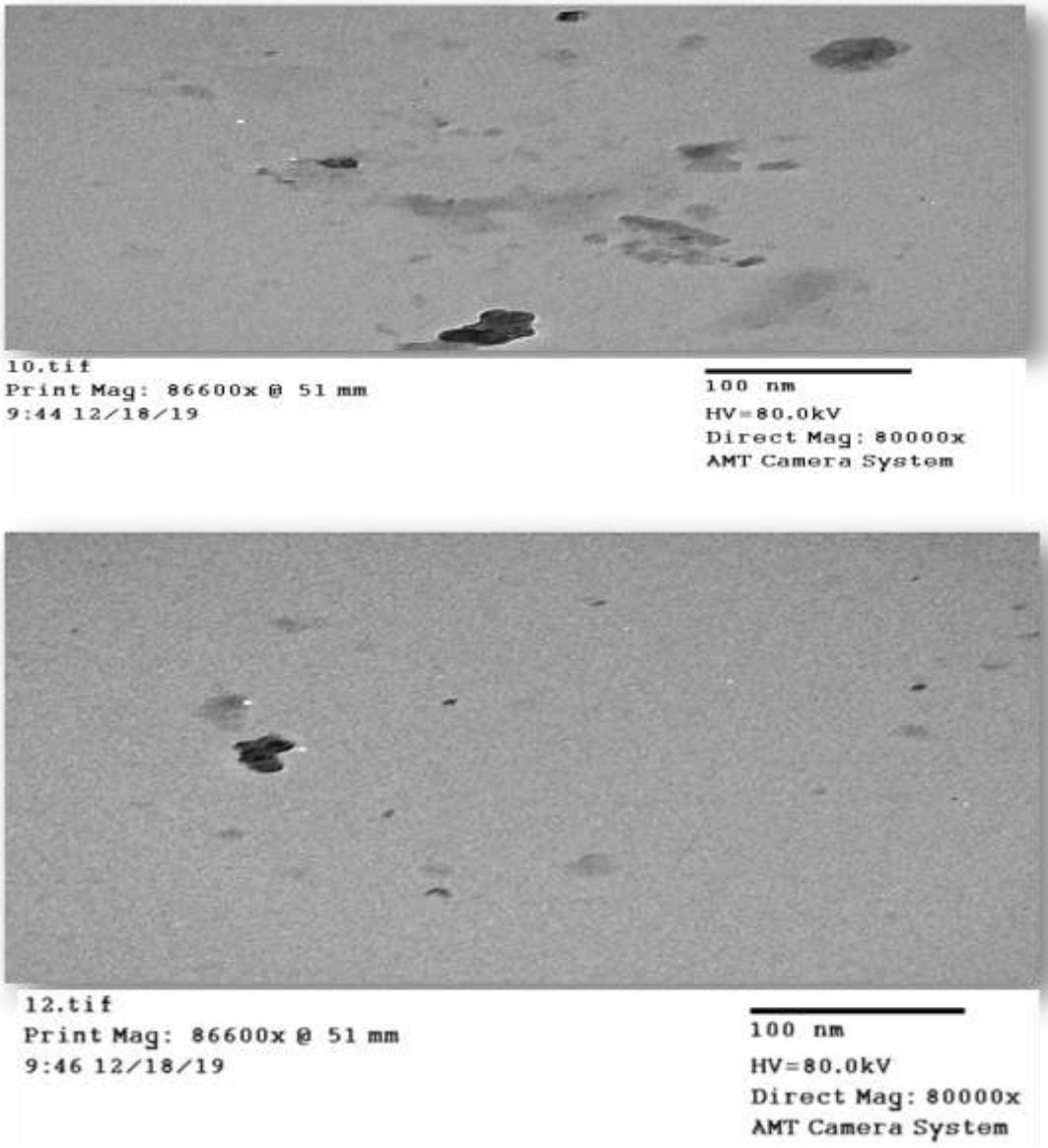

Fig. (1). TEM images of synthesis Graphene Oxide (GO).

2. X-ray diffraction (XRD)

XRD is a highly relevant technique for characterizing intercalation and exfoliation in composites composed of layered materials. So, XRD was chosen to ascertain the GO sheet's typical crystallographic characteristics. Fig. (2) represents the XRD pattern of graphite oxide, which shows that GO displays its unique centered peak at 2θ value 24º which corresponds to an interplanar spacing of (002) hexagonal layers of carbon atoms. Fig. (2) shows that, for the resulted GO, there is a reference to an amorphous band, which is characteristic of non-crystalline materials, for example, monolayer graphene.

However, it is possible to note the existence of little peaks that may be due to the presence of oxygen functional groups and adsorbed water molecules on GO. Subsequently, this image showed the structure of carboxylic acid, phenolic, and hydroxyl groups between graphite nanolayers during the oxidation. Finally, the results of XRD at first demonstrated the fruitful amalgamation and synthesis of GO sheets.

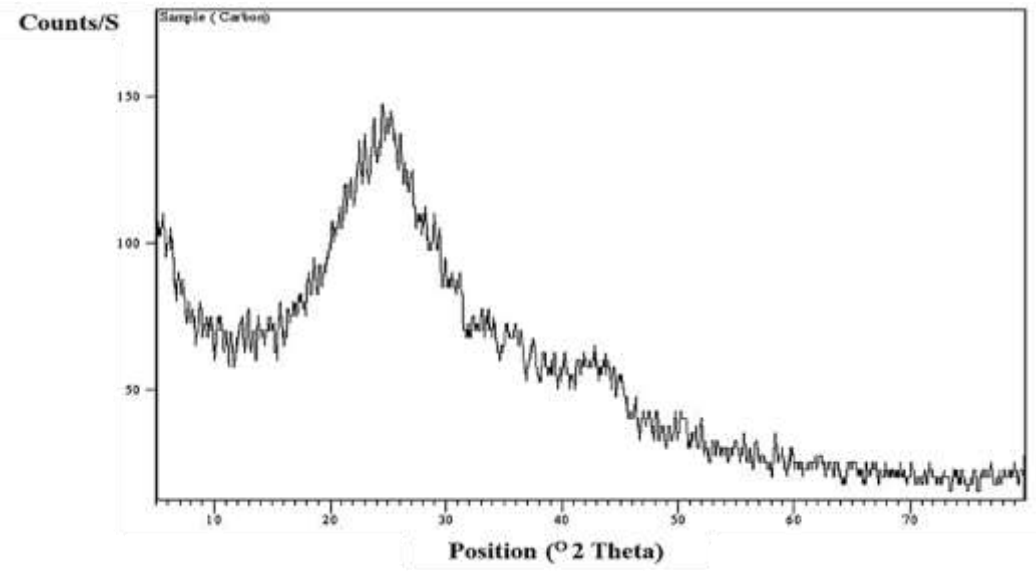

Fig. (2). X-ray diffraction of the Synthesis of Graphene Oxide (GO).

3. Fourier-transform infrared (FT-IR)

The functional groups and design of GO films were investigated using a Fourier-transform infrared spectral analyzer (FT-IR). The FTIR spectra of the GO sheet are depicted in Fig. 3. The data in Fig. (3) demonstrated a wide top in the high-recurrence region between 3000 and 3700 cm^{-1} in comparison to extending as well as the twisting vibration of OH groupings for adsorbed water atoms on GO. In this way, it is assumed that the example has high hydrophilicity. Characteristic peaks for carboxyl C=O in GO were observed at 1735 cm^{-1}

Also, FTIR spectra (Fig. 3) were recorded, and the accompanying practical gatherings were recognized in the example: O-H extending vibrations made a strong band (3427 cm^{-1}), (1719-1740 cm^{-1}) C=O extending vibration from the carboxylic acid and carbonyl gatherings, (1590-1623 cm^{-1}) aromatic C=C from unoxidized sp2 C-C bonds, and epoxy C-O vibrations (1250 cm^{-1}) alkoxy C–O (1051 cm^{-1}) affirms the presence of oxygen-containing functional groups, and hydroxy – OH (3427 cm^{-1}) gatherings. The presence of - CH2 and - CH groups in GO is responsible for the bands at 2932 cm^{-1}. According to the literature, the graphite had obviously been oxidized into GO because it included oxygen-containing functional groups like C=O and C-O. Although the basic structure of layer graphite was still preserved, the addition of C=C bunches showed that even graphite had been oxidized into GO.

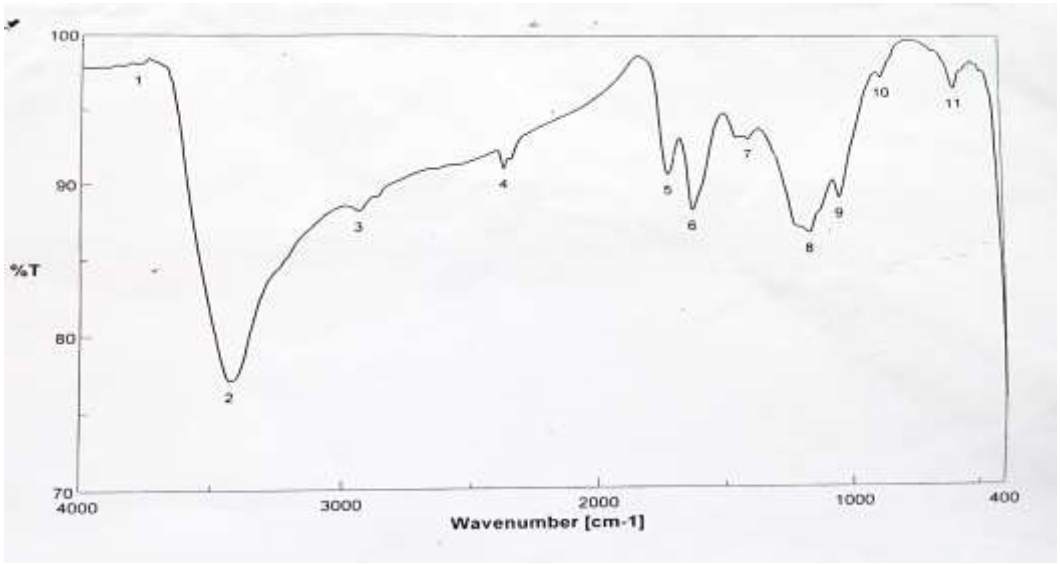

Fig. (3). FT-IR of synthesis graphene oxide (GO).

4. Elemental analysis (EA) of the GO synthesis sheet

The results in Fig. 4 show the data provided in the GO sheet's C element focused on 47.15% during the process of creating the GO sheet using the modified Hummers' technique, which was predictable based on the trial after-effects of the EA inquiry. Furthermore, because of the existence of oxygen-containing practical groups implanted in the GO sheet, H (less than.01%), N (1.02%), and S (0%) were discovered in the sheet of GO. At the same time, as a result of the EA, the oxygen component percentage in the GO film was roughly 51.82%.

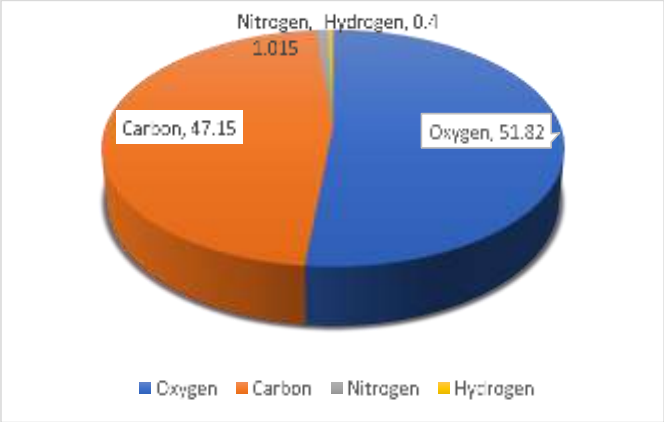

Fig. (4). Elemental's analysis of synthesis graphene oxide (GO).

5. UV–visible spectroscopy

UV-visible spectroscopy is one of the analytical methods used by analytical chemistry to quantitatively characterize various analyses. The UV-noticeable range of graphene oxide consists of a few tops at 218 nm due to the π–π* transition of the C=C bond. In the UV-visible region of graphene oxide, a wide band between 290 and 300 nm is also visible. The C=O band's π–π* transition is responsible for this band.

Additionally, at 231 and 300 nm, respectively, we detected a shoulder and a pinnacle. A study of the diffuse UV-VIS reflectance spectra of the GO sheet is shown in Fig. 5. Graphene oxide is said to exhibit strong absorption in the visible spectrum (198–400 nm), while its absorption in the UV band is also slightly reduced. Data demonstrate the effectiveness of GO sheets under UV or visible light, demonstrating the enormous potential for light utilization.

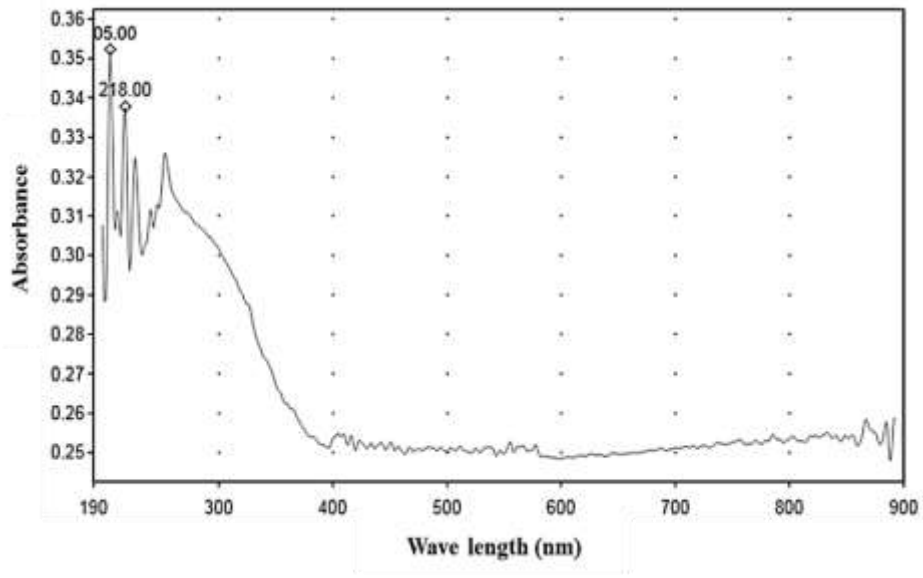

Fig. (5). The UV-VIS spectra of the GO sheet

6. The Atomic Force Microscope (AFM)

Atomic force microscopy (AFM) is used to examine the graphene oxide sheets' thickness and sidelong form. The width of one or more sheets can be measured using a forward line scan across the sheets and substrate, or a histogram of the area of interest in the image can be gathered. The AFM pictures of GO in Fig. 6 unmistakably imply that GO is composed of a few stacked layers.

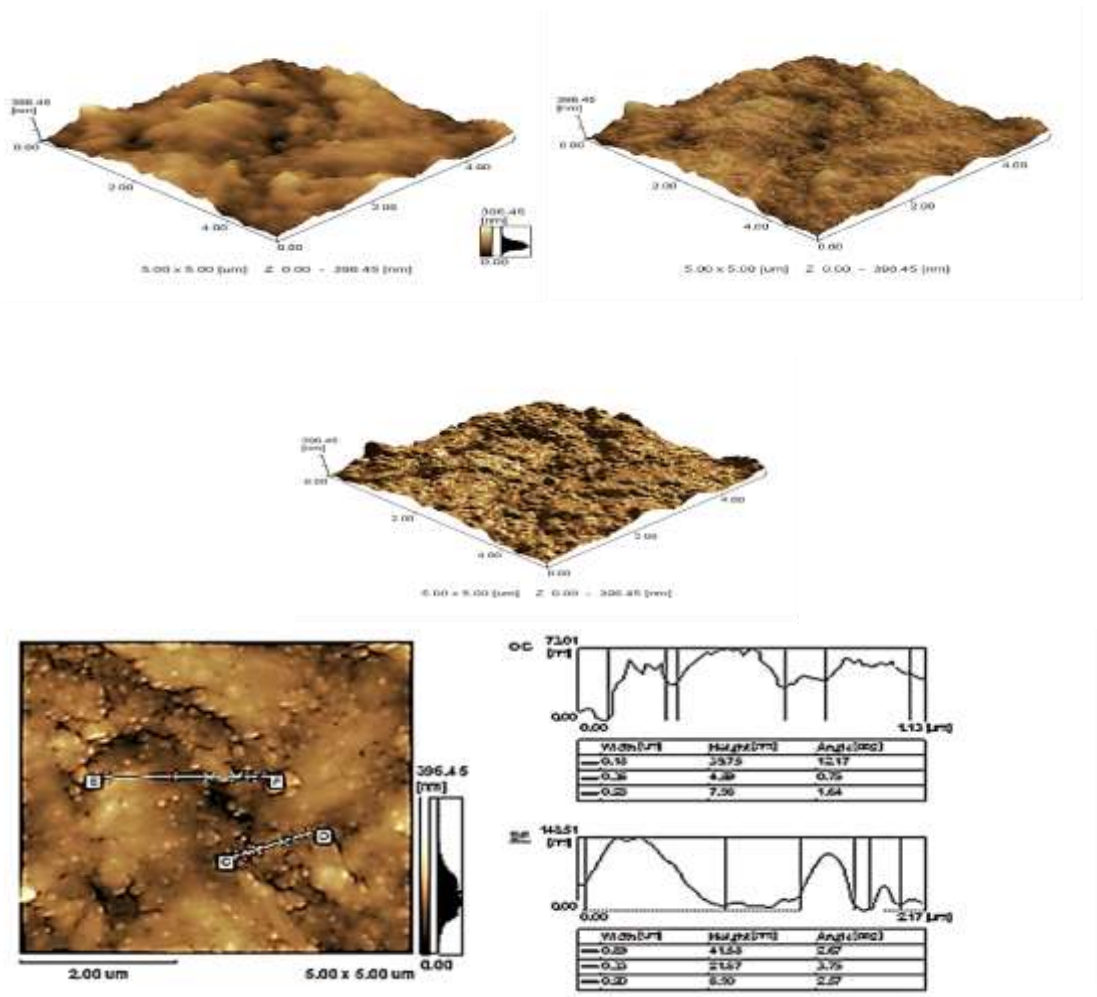

Fig. (6). The images of GO by Atomic Force Microscope (AFM).

7. The Scanning Electron Microscope (SEM)

Fig. 7. shows scanning electron microscopy (SEM) micrographs of GO synthesised using a modified Hummers' preparation. As illustrated in Fig. 7, the GO is composed of two-dimensional sheet-like structures with multiple crinkled and minute layers on the surface. These layers feature inconsistent orchestration and different layering. It has a multi-fold crimpy structure that may be described by adding oxygenated functional groups to the proper architecture, such as hydroxyl, epoxy, and carbonyl groups. The presence of this load of groups allowed carbon to hybridise from sp2 (planar structure) to sp3 (tetrahedral structure).

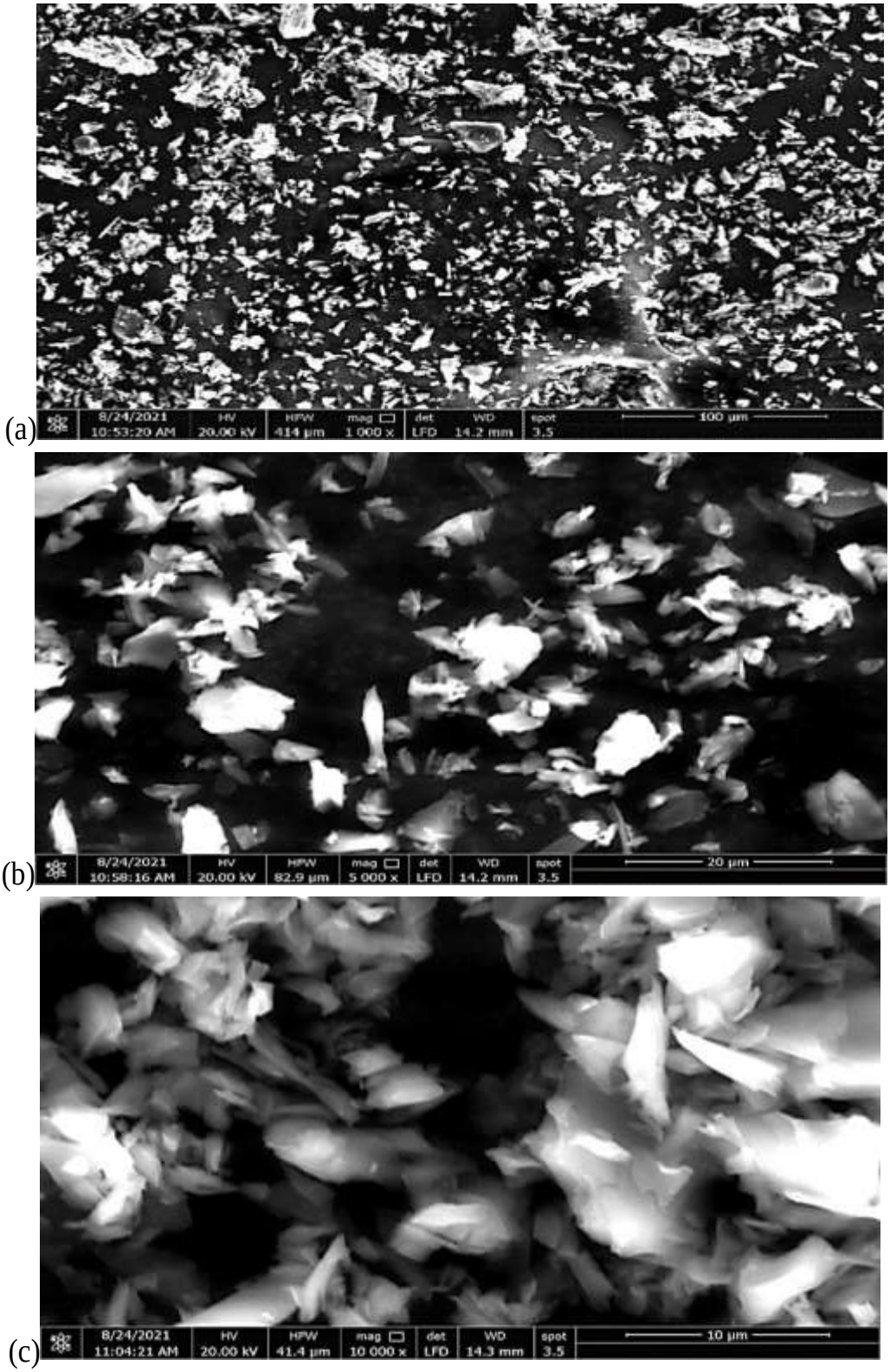

Fig. (7). Scanning Electron Microscope (SEM) images in of GO (a- 1000x, b- 5000x, c- 10000x).

4. Discussion

The synthesis and characterization of graphene oxide have been confirmed by several analyses. According to Shahriary and Athawale (2014), graphite was placed in concentrated acid with an oxidizing agent to produce graphene oxide. Hummers' technique revealed a less hazardous and more effective way to oxidize graphite. The most popular techniques for the oxidation of graphite at the present time are this and modified versions of it (Niyogi et al., 2006; Nakajima et al., 1988). Based on Lerf et al. (1998) and He et al. (1998), individual sheets of GO may be thought of as graphene adorned with oxygen functional groups on both sides of the plane and around the edges. Additionally, Park and Ruoff (2009) demonstrate how graphene oxide's negative surface charge causes electrostatic repulsion between particles, making it very hydrophilic.

When studying the microstructure of GO, Li et al. (2014) and Rourke et al. (2017) used High-Resolution Transmission Electron Microscopy (HR-TEM) and discovered three important components in GO: punctures, graphitic areas, and high-contrast disordered regions, which reveal areas of high oxidation (Erickson et al., 2010). According to Pacilé et al. (2011), puncture formation in GO is induced by the emission of CO and CO_2 during the oxidation processes and sheet exfoliation. Pacilé et al. (2011) revealed that the creation of GO sheets comprises structured zones in addition to problematic oxygen-containing functional group sections. Also,

Guerrero-Fajardo et al. (2020) reported that from these photos, it is clear that monolayers were easily separated from the initial samples. Additionally, there was a significant surface defect that led to irregularities in the plane, indicating that the monolayers' structure was not entirely flat. Thommes et al. (2015) found a direct correlation between the scarcity and the existence of sp3 hybridizing carbons, which resulted in the graphene oxide layers producing epoxy or hydroxyl groups.

The crystalline structure of materials is described via graphene oxide X-ray diffraction investigation. It offers information on the separation between interlayer layers. The XRD technique developed by Kumar and Jalageri (2020) relies on the Braggs rule and interlayer spacing determined by equation (1).

$$\lambda = 2d\sin\theta \qquad (1)$$

λ is the wavelength of the X-ray.
d is the interlayer distance.
θ is the scattering angle.

The interlayer spacing distance of the proper peak, which is visible in the image at a lower angle (2 = 11.30°), is 0.771 nm. There are diffraction peaks at (2 = 26.91°). The entire synthesis of graphene oxide is therefore indicated, and a second noticeable peak at (2 = 26.91°) indicates a 0.330 nm drop in the interlayer spacing distance (Xing et al., 2016). However, (El Achaby et al., 2012; Wojtoniszak et al., 2012) reported that the (002) peak is shifted to a lower angle at 2 = 10.80 following the chemical oxidation and exfoliation into XGO, showing an increase in d-spacing from 0.34 nm to 0.82 nm. The intercalation of oxygen functional groups and water molecules into the carbon layer structure is responsible for an increased interlayer distance between succeeding carbon basal planes.

Furthermore, Sahoo et al. (2021) reported that the presence of graphitic layers in coal is confirmed by a diffraction peak at around a 2h value of 26.05^{O} corresponding to an interlayer spacing (d) of 3.423 with Miller indices (002). The coal powder also has two peaks at 41.51 and 55.97^{O}, which correspond to the (101) and (004) diffraction planes of graphitic layers, respectively [Liu et al., 2008; Saikia et al., 2009]. When compared to neat coal, the distinctive peak of 26.05^{O} became broad and low intensity, indicating higher exfoliation of the graphitic layers into graphene nanolayers (Mastsumoto et al. (2015). The GO exhibits a prominent diffraction peak at about 2 h of 14.26^{O} with an interplanar spacing of 6.2 attributed to the (001) diffraction plane and a wide peak at about 42.25^{O} corresponding to the (100) plane, indicating short-range order in the graphene nanolayers (Johra et al., 2014, Stobinski et al., 2014).

The functional groups and design of GO films were investigated using a Fourier-transform infrared spectral analyzer (FT-IR). In this studied, demonstrated a wide top in the high-recurrence region between 3000 and 3700 cm^{-1} in comparison to extending as well as the twisting vibration of OH groupings for adsorbed water atoms on GO. In this way, it is assumed that the example has high hydrophilicity. Characteristic peaks for carboxyl C=O in GO were observed at 1735 cm^{-1}. Similar results were obtained by Kumar and Jalageri (2020) who reported that FTIR of graphene oxide exhibits broad peaks between 3000-3700 cm^{-1} and another peak due to stretching at 1657.36 cm^{-1}. Bend vibrations of OH of water molecules are absorbed on the surface, giving it a hydrophilic character. The remaining peak, 1108.10 cm^{-1}, belongs to the C-O group of carboxylic acid and the C-OH group of alcohol and relates to the symmetric and asymmetric vibrations of CH_2. This indicates the presence of oxygen, as graphene with functional groups in this group has been entirely oxidized. Graphene oxide's hydrophilic characteristic is due to the creation of hydrogen bonds between graphite and water molecules with hydroxyl groups. Also, Shen et al. (2010) and Chen et al. (2018) found that the significant absorption peaks at 3440 and 1626 cm^{-1} were revealed to corresponded to the vibrations of

absorbed water molecules. Individually, C-O-H deformation and COOH clustering and C=O stretching cause maximal absorbance at 1730 and 1405 cm^{-1}. Because of the epoxy ring distortion and CO, the retention groups at 1060 and 1230 cm^{-1} occur. Previous research, The Vinh et al. (2019) used FT-IR spectroscopy to identify the oxygen functional gatherings of GO. In the GO material, the adsorption band intensities of the C-OH group (3438 cm^{-1}), -C=O (1705 cm^{-1}), C=C (1615 cm^{-1}), =C-H (1400 cm^{-1}), and -C-O-C (1080 cm^{-1}) were solid, indicating more significant substance of hydroxyl groups, alkoxy groups, carboxylic groups, and carbonyl groups, individually (Yu et al., 2016). According to the preceding discussion, both FT-IR and XRD further demonstrated the GO sheets successful synthesis. According to the FTIR data of (Guerrero-Fajardo et al., 2020), the development of a band near 1695 cm^{-1} created by vibrations of the -COOH type (C=O in carboxylic acid) is unequivocal indication that graphene oxide, or GO, was successfully synthesized. The band that corresponds to the C-OH group and appears near 1390 cm^{-1} in addition to 3470 cm^{-1} attributed to the alcohol OH group type in contrast to the - COOH collects and the OH bunches adsorption on the GO surface is one of the many groups that demonstrated the successful processing of the GO. Furthermore, CO group vibrations in the functions of carboxylic acid or epoxy groups on the GO surface introduced a band near 1075 cm^{-1} and C=O vibrations near 1675 cm^{-1} (Muniyalakshmi et al., 2020). In addition, Ossonon and Bélanger (2017) reported that the GO displays absorption bands linked to C-O stretching (1053 cm^{-1}), C-O-C bending (1170 cm^{-1}), C-O-H stretching (1350 cm^{-1}), and C=C stretching from unoxidized graphitic domain (1627 cm^{-1}) vibrations. The C=O stretching (1714 cm^{-1}) mode corresponds to carboxylic acid and carbonyl functionalities, which are mostly present on the graphene sheets' basal plane and at their edges. According to Emiru and Ayele (2017), the peaks at 2974 and 2866 cm-1 represent the asymmetric and symmetric methylene (CH2) C-H stretching of GO, respectively. The GO exhibits a broad absorption peak between 3000 and 3500 cm^{-1}, which is associated with the -OH stretching vibration of carboxylic (-COOH) groups and absorbed water molecules. The presence of hydroxyl (-OH), carboxylic (-COOH), and epoxy functional groups on the surface of graphene nanosheets is confirmed by FTIR analysis (Dreyer et al., 2010 and Lomeda et al., 2008). Finally, the existence of these groups containing oxygen indicates that the graphite has been oxidized. The polar groups, particularly the surface hydroxyl groups, cause hydrogen bonds to form between graphite and water molecules, which explains graphene oxide's hydrophilic characteristic.

Results supplied in the GO sheet's C element were 47.15% during the construction process using the modified Hummers' technique. The detection of H (less than 0.1%), N (1.02%), and S (0%) in the GO sheet was also influenced by the presence of oxygen-containing practical groups implanted in the GO sheet. At the same time, the EA caused the oxygen component percentage in the GO film to be roughly 51.82%. According to Botas et al. (2013), graphite contains 98% carbon by weight. Due to the carbon being replaced by oxygenated groups following the oxidation process, the amount of carbon in GO samples was significantly smaller than in graphite. It has been established that the majority of oxygen is present as hydroxyl, epoxy, and carboxyl groups, which are found near the borders of the sheets and inside the aromatic domains. GrO produced using the optimized process had a little lower oxygen concentration and higher sulphur and nitrogen in its structure, according to an elemental analysis. The amount of residual components in the sample increased as a result of the cleaning step's reduction from two to one wash, according to the last piece of information.

Song et al. (2014) added that the increased mass of pure graphite during the process of manufacturing the GO sheet using the modified Hummers' method was 5.0g, and the ultimate quantity of the created GO sheet was approximately 11.1 g. We can theoretically infer that the C element content in the GO sheet was around 45.0%, which was consistent with the experimental results of the EA analysis, which showed that H (3%) and S (0.9%) were observed in the GO sheet, owing to the presence of oxygen-containing functional groups embedded in the GO sheet. Meanwhile, according to the EA data, the O element content in the GO film was approximately 51%.

UV–visible spectroscopy

Analytical chemistry employs UV-visible spectroscopy as one of its analytical methods for quantitatively characterising diverse results. The UV-visible range of graphene oxide consists of a few tops at 218 nm caused by the C=C bond's π–π*transition. A broad band between 290 and 300 nm is observed in the UV-visible region of graphene oxide. This band is caused by the π–π*transition in the C=O band. Additionally, at 231 and 300 nm, respectively, we detected a shoulder and a pinnacle. A study of the diffuse UV-VIS reflectance spectra of the GO sheet is shown in Fig. 5. Graphene oxide is said to exhibit strong absorption in the visible spectrum (198–400 nm), while its absorption in the UV band is also slightly reduced. Data demonstrate the effectiveness of GO sheets under UV or visible light, demonstrating the enormous potential for light utilisation. According to Lai et al. (2012) and Khan (2017), the strength of the peak at 230 nm in the UV-

visible spectrum of graphene oxide declines as layers number rises. However, Guerrero-Fajardo et al. (2020) found that GO had two distinct bands: one at 235 nm, which was brought on by a change in the electrons' π–π* transition inside the C-C aromatic bond of the graphene layers, and the other, a shoulder-like band at 306 nm, which was linked to the π–π* transition and was brought on by the oxygen content. Fernández-Merino et al. (2010), Lee et al. (2010), and (Kigozi et al., 2020) all came to similar conclusions. According to the absorbance spectra, The main spectrum of GO has an absorption peak at 230nm, attributed to π-$\pi*$ transition of the aromatic C–C ring and weak absorption at 303 nm due to π-$\pi*$ transition of C=O bond (El Achaby et al., 2012 ; Thakur and Karak , 2012).Recently, Sahoo et al., 2021) found that the absorption peak centered at around λmax = 235 nm resembles π-π*transition for C=C double bond of graphene layers (Ossonon and Bélanger 2017; Li et al.,2008). A shoulder observed at around 300 nm is attributed to π–π*transition because of the C-O and C=O groups present on the graphene sheets (Marcano et al., 2010). The UV-Vis spectrum shows the higher value of λmax for π-π*electronic transition as compare to π–π*because the π-π* transitions require less amount of energy due to the conjugation of C=C bonds of the graphene layers.

The thickness and sidelong shape of graphene oxide sheets are examined using atomic force microscopy (AFM). A forward line scan across the sheets and substrate can be used to measure the width of one or more sheets, or a histogram of the area of interest in the image can be obtained. The AFM images of GO in Fig. 6 clearly show that it is made up of a few stacked layers. The results generally agree with those of Alam et al. (2017; Malas et al. (2012). In addition, Khan (2017) and Mkhoyan et al., (2009) said that the thickness of graphene oxide sheets is frequently greater than that of graphene. The presence of multiple groups attached to the graphene lattice results in increased graphene oxide thickness.

SEM is used to obtain the inner morphology of GO. Fig. 7 shows a picture of the microstructure of a produced sample at a SEM magnification of 13k. Particle size reduction was found to have a substantial effect on GO and the layering of graphite stacks. The layers within the layers are further dissected, revealing a curlier structure. This is the result of increased surface area (as a result of particle size reduction), which allows for efficient oxidation during the process (Kumar and Jalageri, 2020). Additionally, as the substance oxidized, the transitional distance between the graphite layers grew. (Muniyalakshmi et al., 2020; Şahin et al., 2020) found similar data. Furthermore, the SEM images of the GO (Fig.7) revealed modest translucence, showing that there were not many layers, also, however had coarse and tucked regions (Guerrero-Fajardo et al., 2020). To put it another way, it was discovered that the individual GO sheets had a thickness of 1 to 2 m, which is considerably thicker than graphene's single layer. Due to the presentation of practical gatherings that contain oxygen, the thickness has increased. Additionally, it was observed that the borders of the GO sheets were thicker. The oxygen-containing functional groups were primarily concentrated close to the margins of GO, which explains this. The SEM photos (Alam et al., 2017) and (Abaszade et al., 2021) show that the GO sheets were immovably suspended and did not flex. According to Sahoo et al. (2021), the SEM pictures are exhibited at low resolution (x1000), yet the change in morphology is also noticed to some extent. The coal sample contains microscopic granular particles that are not homogeneous in size. However, the aggregate structures of GO and graphene nanosheets are globular in size. The morphology of the coal changes considerably as a result of the chemical methods used to synthesis graphene nanolayers. In comparison to coal, graphene nanosheets have a rippled surface, uniformly distributed particles, and porous architectures, resulting in non-homogeneously organized aggregates that are strongly coupled to produce an irregular solid shape (Siburian et al., 2018).

Environmental applications of GO

Nanomaterials are chemical compounds with nanosized particles ranging in size from 1 to 100 nm. They have unique properties such as increased strength, high chemical reactivity, and electrical conductivity. Nanotechnology uses nanomaterials to build stronger, lighter, cheaper, more durable, and more precise goods in a variety of industries, including industrial manufacturing, medical, medication delivery, food, and consumables. However, there are also concerns about health and safety, pollution, military upgrades, environmental consequences, and nanotoxicity. Carbon nanomaterials, particularly carbon nanoparticles, have substantial environmental and human health impacts, with severe biological consequences and potential harm to human life Sahoo et al. (2021). However, Jiˇríˇcková et al. (2022) noted that due to industrial discharges of hazardous gases such as CO_2, CO, NO_2, and NH_3, air pollution is a significant environmental threat. Because of its oxygen groups, GO may interact with a wide range of molecules and be employed in catalysis to transform harmful gases during industrial processes (Li et al., 2015). GO can also be used to combat water pollution, which is a major environmental issue. Pollutant adsorption and conversion are two types of GO uses. Few-layered GO composites exhibit distinct adsorption behavior towards CO_2 and hazardous gases, with laminar

architectures containing rapid and selective gas separation channels. Yumura and colleagues (2014) found that GO-based composites can also adsorb additional hazardous gases such as acetone (Zhou et al., 2014) and formaldehyde (Esrafili and colleagues, 2018). According to Jankovský et al. (2015), graphene oxide (GO) has a great capacity for adsorbing heavy metals, making it essential for the filtration of water. Few-layered graphene oxide nanosheets exhibit a strong affinity for Pb (II) ions, according to research on their ability to adsorb across the periodic table (Zhao et al., 2011). However, even with oxygen groups on GO serving as active sites, Cu2+ adsorption capability is poor. Yang et al. (2010). With the aid of organic molecules, GO can offer more practical anchoring sites for heavy metal ions (Qi et al., 2017). Additionally, it absorbs organic dyes, with methyl orange not being absorbed while methylene blue and rhodamine B show quick selectivity (Molla et al., 2019).

On the other hand, climate change is a global issue affecting weather events, temperature rise, flooding, precipitation patterns, droughts, heat stress, and sea level rise (Elbasiouny and Elbehiry, 2020; El-Ramady et al., 2021). Soil carbon plays a crucial role in mitigating climate change and maintaining soil health in agro-ecosystems (Li et al., 2019). Accurate assessment of C stocks and distributions is essential for mitigating emissions and improving understanding of soil responses to climate change. Soil C and nitrogen sequestration are essential for mitigating greenhouse gas emissions and improving soil quality, according to Elbasiouny and Elbehiry (2019). Also, climate change affects global soil organic carbon (SOC) stocks (Soleimani et al., 2017), and a slight change in soil C stocks significantly impacts atmospheric CO_2 concentration (Li et al., 2019). Carbon capture through photosynthesis and decomposition of plants, residues, soil fauna, and microbes is vital for living organisms. Climate change has significantly impacted plant nutrition, food security (Liu et al., 2020; Krüger et al., 2021), Kumar et al. (2022), and plant-herbivore interactions. As a result, future crops with climate-resilient plant immune systems are needed to address these challenges by using different strategies, including nanotechnology, especially nanocarbon, to ensure the sustainability of cultivated plants and food security.

5. CONCLUSION

Graphene oxide (GO) was effectively prepared with a modified Hummers' method by oxidizing purified natural flake graphite. Because oxygen-containing functional groups were connected at the borders of the GO, it was discovered that the GO was composed of stacks of GO sheets and was thicker there. Numerous tests (including TEM, XRD, FT-IR, EA, UV, AFM, and SEM) revealed that the indicated method was successful in producing the GO films. According to the TEM analysis, the GO films are effectively generated by microscopic morphology. The existence of oxygen-containing groups and distinct peaks in XRD and FT-IR measurements determined the effectiveness of GO sheet manufacturing. The sample comprises various functional groups in the FT-IR spectra, including hydroxyl, carboxyl, carbonyl, and epoxy. EA also revealed that the oxygen component in GO films was roughly 51.8%; components of C, H, and N were also discovered. Furthermore, the existence of oxygen-containing functional groups broadened GO's potential uses in a variety of fields. UV-vis studies revealed that graphene oxide absorbs well in the visible range (198~400 nm). The thickness and parallel morphology of graphene oxide sheets are investigated using AFM. Finally, SEM revealed a surface framed by crinkled and thin layers. This information will serve as a link to a more in-depth examination of the concept of graphene oxide.

Conflicts of interest

There are no conflicts to declare.

6. References

Abaszade RG, Mamedova SA, Agayev FG, Budzulyak SI, Kapush OA, Mamedova MA, Nabiyev A M, Kotsyubynsky VO (2021). Synthesis and characterization of graphene oxide flakes for transparent thin films. Physics and Chemistry of Solid State, 22(3), 595–601.

Alam SN, Sharma N, Kumar L (2017). Synthesis of Graphene Oxide (GO) by Modified Hummers Method and Its Thermal Reduction to Obtain Reduced Graphene Oxide (rGO)*. Graphene, 06(01), 1–18.

Avdeev VV, Monyakina LA, Nikolskaya IV, Sorokina NE, Semenenko KN (1992). The choice of oxidizers for graphite hydrogenosulfatechemical synthesis. Carbon, 30, 819–823. [CrossRef]

Badgar K, Prokisch J, El-Ramady H (2021). Nanofibers for Sustainable Agriculture: A Short Communication. Egypt. J. Soil Sci. Vol. 61, No. 3, pp. 373 – 380 DOI: 10.21608/ejss.2021.105877.1477.

Botas C, Álvarez P, Blanco C, Santamaría R, Granda M, Gutiérrez MD, Rodríguez-Reinoso F, Menéndez R (2013). Critical temperatures in the synthesis of graphene-like materials by thermal exfoliation-reduction of graphite oxide. Carbon, 52, 476-485.

Bystrzejewski M, Cudziło S, Huczko A, Lange H, Soucy G, Cota-Sanchez G, Kaszuwara W (2007). Carbon encapsulated magnetic nanoparticles for biomedical applications: Thermal stability studies. Biomolecular Engineering, 24(5), 555–558.

Chen L, Yang S, Liu Y, Mo M, Guan X, Huang L, Sun C, Yang ST, Chang XL (2018). Toxicity of graphene oxide to naked oats (Avena sativa L.) in hydroponic and soil cultures †.

Dreyer DR, Park S, Bielawski CW, Ruoff RS (2010). The chemistry of graphene oxide. Chem. Soc. Rev. 39, 228–240.

Dubin S, Gilje S, Wang K, Tung VC, Cha K, Hall AS, Farrar J, Varshneya R, Yang Y, Kaner RB (2010). A one-step, solvothermal reduction method for producing reduced graphene oxide dispersions in organic solvents. ACS Nano, 4(7), 3845–3852.

Eigler S, Hirsch A (2014). Chemistry with graphene and graphene oxide - Challenges for synthetic chemists.AngewandteChemie - International Edition .53, 2–21

El Achaby M, Arrakhiz FZ, Vaudreuil S, Essassi EM, Qaiss A (2012). Piezoelectric β-polymorph formation and properties enhancement in graphene oxide—PVDF nanocomposite films. Applied Surface Science, vol. 258, no. 19, pp. 7668–7677.

Elbasiouny H, Elbehiry F (2019). Soil Carbon and Nitrogen Stocks and Fractions for Improving Soil Quality and Mitigating Climate Change: Review. Egypt. J. Soil. Sci. Vol. 59, No. 2, pp. 131- 144

Elbasiouny H, Elbehiry F (2020). Rice Production in Egypt: The Challenges of Climate Change and Water Deficiency. In: Ewis Omran ES., Negm A. (Eds) Climate Change Impacts on Agriculture and Food Security in Egypt. Springer Water, Springer, Cham. https://doi.org/10.1007/978-3-030-41629-4_14

El-Ramady H, El-Mahdy S, Awad A, Nassar S, Osman O, Metwally E, Aly E, Fares E, El-Henawy A (2021). Is Nano-Biofortification the Right Approach for Malnutrition in the Era of COVID-19 and Climate change? Egypt. J. Soil. Sci. 61 (2), 161-173. DOI: 10.21608/ejss.2021.75653.1445

El-shahawy A, El-Refaey A, Ibrahim M, Abd El-Halim A, Talha N, Mahmoud E (2022). Effect of nanomaterials on Soil Quality and Yield of Canola (Brassica napus L.) Grown in Heavy Clayey Soils. Egypt. J. Soil Sci. Vol. 62, No. 4, pp: 361 – 371

Emiru TF, Ayele DW (2017). Controlled synthesis, characterization and reduction of graphene oxide: A convenient method for large scale production. Egyptian Journal of Basic and Applied Sciences, 4(1), 74-79.

Erickson K, Erni R, Lee Z, Alem N, Gannett W, Zettl A (2010). Determination of the local chemical structure of graphene oxide and reduced graphene oxide. Advanced Materials, 22(40), 4467–4472.

Esrafili MD, Dinparast L (2018). The selective adsorption of formaldehyde and methanol over Al-or Si-decorated graphene oxide: A DFT study. J. Mol. Graph. Model. 80, 25–31. [CrossRef]

Fernández-Merino MJ, Guardia L, Paredes JI, Villar-Rodil S, Solís-Fernández P, Martínez-Alonso A, Tascón JMD (2010). Vitamin C is an ideal substitute for hydrazine in the reduction of graphene oxide suspensions. Journal of Physical Chemistry C, 114(14), 6426–6432.

Ghazi Dina A, Abbas AY, Abdelghany A M, El-Sherpiny MA, El-Ghamry AM (2022). Evaluating Nanotechnology in Raising the Efficiency of some Substances Used in Fertilizing Wheat Grown on Sandy Soil. Egyptian Journal of Soil Science Vol. 62, No. 2, pp. 123 – 135

Guerrero-Fajardo CA, Giraldo L, Moreno-Piraján JC (2020). Preparation and characterization of graphene oxide for Pb (II) and Zn (II) ions adsorption from aqueous solution: Experimental, thermodynamic and kinetic study. Nanomaterials, 10(6).

He H, Klinowski J, Forster M, Lerf A (1998). A new structural model for graphite oxide. Chem. Phys. Lett. 287, 53-56.

Huang X, Yin Z, Wu S, Qi X, He Q, Zhang Q, Yan Q, Boey F, Zhang H (2011). Graphene-based materials: synthesis, characterization, properties, and applications, Small 1876 1902

Hummers WS, Offeman RE (1958). Preparation of Graphitic Oxide. Journal of the American Chemical Society, 80(6), 1339.

Jankovský O, Šimek P, Klímová K, Sedmidubský D, Pumera M, Sofer Z (2015). Highly selective removal of Ga3+ ions from Al3+/Ga3+ mixtures using graphite oxide. Carbon 89, 121–129. [CrossRef]

Jiˇrí ˇcková A, Jankovský O, Sofer Z, Sedmidubský D (2022). Synthesis and Applications of Graphene Oxide. Materials, 15, 920. https:// doi.org/10.3390/ma15030920

Johra FT, Lee JW, Jung WG (2014). Facile and safe graphene preparation on solution-based platform J. Ind. Eng. Chem. 20, 2883–2887.

Khan ZH (2017). Advanced Structured Materials Recent Trends in Nanomaterials Synthesis and Properties. http://www.springer.com/series/8611

Kiang Chua C, Pumera M (2014). Chemical reduction of graphene oxide: a synthetic chemistry viewpoint. Chem. Soc. Rev, 43, 291.

Kigozi M, Koech RK, Kingsley O, Ojeaga I, Tebandeke E, Kasozi GN, Onwualu AP (2020). Synthesis and characterization of graphene oxide from locally mined graphite flakes and its supercapacitor applications. Results in Materials, 7, 100113.

Krüger I, Schmitz A, Sanders TG (2021). Climate condition affects foliar nutrition in main European tree species. Ecological Indicators, 130, 108052. doi: 10.1016/j.ecolind.2021.108052

Kumar GC, Jalageri M (2020). Synthesis and characterization of graphene oxide by modified hummer method. AIP Conference Proceedings 2247, 040018, https://doi.org/10.1063/5.0003864

Kumar V, Srivastava A, Suprasanna P (2022). Plant Nutrition and Food Security in the Era of Climate Change. 1st edition Academic Press, https://doi.org/10.1016/C2019-0-04692-4

Lai Q, Zhu S, Luo X, Zou M, Huang S (2012). Ultraviolet-visible spectroscopy of graphene oxides. AIP Advances, 2(3). https://doi.org/10.1063/1.4747817

Lee DW, De Los Santos V L, Seo JW, Leon Felix L, Bustamante D A, Cole JM, Barnes CH. (2010). The structure of graphite oxide: Investigation of its surface chemical groups.

Lerf A, He H, Forster M, Klinowski J (1998). Structure of Graphite Oxide Revisited. J. Phys. Chem. B 102, 4477-4482.

Li B, Cao H, Shao J, Qu M, Warner JH (2011). Superparamagnetic Fe3O4 nanocrystals@graphene composites for energy storage devices. Journal of Materials Chemistry, 21(13), 5069–5075.

Li D, Mueller MB, Gilje S, Kaner RB, Wallace GG (2008). Processable aqueous dispersions of graphene nanosheets. Nat. Nanotechnol. 3,101–105.

Li F, Jiang X, Zhao J, Zhang S (2015). Graphene oxide: A promising nanomaterial for energy and environmental applications. Nano Energy, 16, 488–515. [CrossRef]

Li J, Zeng X, Ren T, Van Der Heide E (2014). The Preparation of Graphene Oxide and Its Derivatives and Their Application in Bio-Tribological Systems. 2, 137–161.

Li M, Han X, Du S, Li L (2019). Profile stock of soil organic carbon and distribution in croplands of Northeast China. Catena, 174, 285–292. https:// doi.org/10.1016/j.catena. 2018.11.027.

Liu BN, Luo F, Wu H, Liu Y, Zhang Ch (2008). One-Step Ionic-Liquid-Assisted Electrochemical Synthesis of Ionic-Liquid-Functionalized Graphene Sheets Directly from Graphite J. Chen, Adv. Funct. Mater. 18, 1518–1525.

Liu C, Zou D, Li Y (2020). Nutrient availability modulates the effects of climate change on growth and photosynthesis of marine macroalga Pyropia haitanensis (Bangiales, Rhodophyta). Journal of Applied Phycology 32, 3285–3294. https://doi.org/10.1007/s10811-020-02189-y

Lomeda JR, Doyle CD, Kosynkin DV, Hwang WF, Tour JM (2008). Diazonium Functionalization of Surfactant-Wrapped Chemically Converted Graphene Sheets J. Am. Chem. Soc. 130, 16201–16206.

Luo Z, Lu Y, Somers LA, Johnson ATC (2009). High yield preparation of macroscopic graphene oxide membranes. Journal of the American Chemical Society, 131(3), 898–899.

Malas A, Das CK, Das A, Heinrich G (2012). Development of expanded graphite filled natural rubber vulcanizates in presence and absence of carbon black: Mechanical, thermal and morphological properties. Materials and Design, 39, 410–417.

Mani PK, Mondal S (2016). Agri-nanotechniques for plant availability of nutrients. In: C. Kole et al. (eds.), Plant Nanotechnology (pp. 263-303). Springer, Cham. 10.1007/978-3-319-42154-4_11

Marcano DC, Kosynkin DV, Berlin JM, Sinitskii A, Sun Z, Slesarev A, Alemany LB, Lu W, Tour JM (2010). Improved synthesis of graphene oxide. ACS Nano, 4(8), 4806–4814.

Matsumoto M, Saito Y, Park C, Fukushima T, Aida T (2015). Ultrahigh-throughput exfoliation of graphite into pristine 'single-layer' graphene using microwaves and molecularly engineered ionic liquids Nat. Chem. 7,730–736.

Méndez-Lozano N, Pérez-Reynoso F, González-Gutiérrez C (2022). Eco-Friendly Approach for Graphene Oxide Synthesis by Modified Hummers Method. Materials 15, 7228. https://doi.org/10.3390/ ma15207228

Mkhoyan KA, Contryman AW, Silcox J, Stewart DA, Eda G, Mattevi C, Miller S, Chhowalla M (2009). Atomic and electronic structure of graphene-oxide. Nano Letters, 9(3), 1058–1063.

Molla A, Li Y, Mandal B, Kang SG, Hur SH, Chung JS (2019). Selective adsorption of organic dyes on graphene oxide: Theoretical and experimental analysis. Appl. Surf. Sci. 464, 170–177. [CrossRef]

Morishige K, Hamada T (2005). Iron Oxide Pillared Graphite. Langmuir, 21(14), 6277–6281.

Muniyalakshmi M, Sethuraman K, Silambarasan D (2020). Synthesis and characterization of graphene oxide nanosheets. Materials Today: Proceedings, 21, 408–410.

Nakajima T, Mabuchi A, Hagiwara R (1988). A new structure model of graphite oxide. Carbon 26, 357-361.

Niyogi S, Bekyarova E, Itkis ME, McWilliams JL, Hamon MA, Haddon RC (2006). Solution properties of graphite and graphene. J. Am. Chem. Soc. 1287720-21.

Ossonon BD, Bélanger D (2017). Synthesis and characterization of sulfophenyl-functionalized reduced graphene oxide sheets RSC Adv. 7, 27224–27234.

Pacilé D, Meyer JC, Fraile Rodríguez A, Papagno M, Gómez-Navarro C, Sundaram RS, Burghard M, Kern K, Carbone C, Kaiser U (2011). Electronic properties and atomic structure of graphene oxide membranes. Carbon, 49(3), 966–972.

Paredes JI, Villar-Rodil S, Martínez-Alonso A, Tascón JMD (2008). Graphene oxide dispersions in organic solvents. Langmuir, 24(19), 10560–10564.

Park S, Ruoff RS (2009). Chemicalmethods for the production of graphenes. Nature Nanotechnology, vol. 5, no. 4, pp. 217–224.

Pendolino F, Armata N (2017). SPRINGER BRIEFS IN APPLIED SCIENCES AND TECHNOLOGY Graphene Oxide in Environmental Remediation Process.

Pramanik P, Ray P, Maity A, Das S, Ramakrishnan SS, Dixit P (2020). Nanotechnology for Improved Carbon Management in Soil. P. K. Ghosh et al. (Eds.), Carbon Management in Tropical and Sub-Tropical Terrestrial Systems, https://doi.org/10.1007/978-981-13-9628-1_24, pp: 403 – 415. Springer Nature Singapore Pte Ltd.

Qi Y, Yang M, Xu W, He S, Men Y (2017). Natural polysaccharides-modified graphene oxide for adsorption of organic dyes from aqueous solutions. J. Colloid Interface Sci. 486, 84–96. [CrossRef]

Rourke JP, Pandey PA, Moore JJ, Bates M, Kinloch IA, Young RJ, Wilson NR (2011). Graphene Oxide the Real Graphene Oxide Revealed: Stripping the Oxidative Debris from the Graphene-like Sheets**.

Şahin S, Ciğeroğlu Z, Özdemir OK, Elhussein E, Gülmez Ö (2020). Investigation of graphene oxide as highly selective adsorbent in recovery of hydroxytyrosol from olive mill wastewater. International Journal of Environmental Science and Technology, 17(12), 4803–4814.

Sahoo P, Shubhadarshinee L, Jali BR, Mohapatra P, Barick AK (2021). Synthesis and characterization of graphene oxide and graphene from coal, Materials Today: Proceedings, https://doi.org/10.1016/j.matpr.08.206

Saikia BK, Boruah RK, Gogoi PK (2009). An X-ray diffraction analysis on graphene layers of Assam coal J. Chem. Sci. 121, 103–106.

Seyed H, Shabnam B (2017). Graphene Oxide/Zinc Oxide (GO/ZnO) Nanocomposite as a Superior Photocatalyst for Degradation of Methylene Blue (MB)-Process Modeling by RSM. Journal of the Brazilian Chemical Society. 28, 203-207

Shahriary L, Athawale A A (2014). Graphene Oxide Synthesized by using Modified Hummers Approach. International Journal of Renewable Energy and Environmental Engineering Vol. 02, No. 01. pp 58-63.

Shan SJ, Zhao Y, Tang H, Cui FY (2017). A Mini-review of Carbonaceous Nanomaterials for Removal of Contaminants from Wastewater. IOP Conference Series: Earth and Environmental Science, 68(1).

Shen X, Wu J, Bai S, Zhou H (2010). One-pot solvothermal syntheses and magnetic properties of graphene-based magnetic nanocomposites. Journal of Alloys and Compounds, 506(1), 136–140.

Shin YR, Jung SM, Jeon IY, Baek JB(2013). The oxidation mechanism of highly ordered pyrolytic graphite in a nitric acid/sulfuric acid mixture. Carbon, 52, 493–498. [CrossRef]

Siburian R, Sihotang H, Raja SL, Supeno M, Simanjuntak C (2018). New Route to Synthesize of Graphene Nano Sheets. J. Chem. 34 182–187.

Singh DP, Herrera CE, Singh B, Singh S, Singh RK, Kumar R (2018). Graphene oxide: An efficient material and recent approach for biotechnological and biomedical applications. Mater Sci Eng C Mater Biol Appl. May 1; 86:173-197. doi: 10.1016/j.msec.2018.01.004. Epub 2018 Feb 1. PMID: 29525091.

Singh RK, Kumar R, Singh DP (2016). Graphene oxide: strategies for synthesis, reduction, and frontier applications, RSC Advances.6 ,64993–65011

Smith AT, LaChance AM, Zeng S, Liu B, Sun L (2019). Synthesis, properties, and applications of graphene oxide/reduced graphene oxide and their nanocomposites. Nano Materials Science, 1(1), 31–47.

Soleimani A, Hosseini SM, Bavani ARM, Jafari M, Francaviglia R (2017). Simulating soil organic carbon stock as affected by land cover change and climate change, Hyrcanian forests (northern Iran). Science of the Total Environment ,599-600, 1646-1657.

Sorokina NE, Khaskov MA, Avdeev VV, Nikol'skaya IV (2005). Reaction of graphite with sulfuric acid in the presence of KMnO4. Russ. J. Gen. Chem., 75, 162–168. [CrossRef]

Song J, Wang X, Chang CT (2014). Preparation and characterization of graphene oxide. Journal of Nanomaterials, 2014. https://doi.org/10.1155/2014/276143

Stankovich S, Dikin DA, Piner RD, Kohlhaas KA, Kleinhammes A, Jia Y, Wu Y, Nguyen SBT, Ruoff RS (2007). Synthesis of graphene-based nanosheets via chemical reduction of exfoliated graphite oxide. Carbon, 45(7), 1558–1565.

Stobinski L, Lesiak B, Malolepszy A, Mazurkiewicz M, Mierzwa B, Zemek J, Jiricek P, Bieloshapka I (2014) Graphene Oxide and Reduced Graphene Oxide Studied by the XRD, TEM and Electron Spectroscopy Methods. Journal of Electron Spectroscopy and Related Phenomenon, 195, 145-154. https://doi.org/10.1016/j.elspec.2014.07.003

Thakur S, Karak N (2012). Green reduction of graphene oxide by aqueous phytoextracts. Carbon, vol. 50, no. 14, pp. 5331–5339.

The Vinh L, Ngoc Khiem T, Dang Chinh H, Van Tuan P, Tan VT (2019). Adsorption capacities of reduced graphene oxide: effect of reductants. Materials Research Express, 6(7), 075615.

Thommes M, Kaneko K, Neimark AV, Olivier JP, Rodriguez-Reinoso F, Rouquerol J, Sing KSW (2015). Physisorption of gases, with special reference to the evaluation of surface area and pore size distribution (IUPAC Technical Report). Pure and Applied Chemistry, 87(9–10), 1051–1069.

Wang X, Shi G (2015). An introduction to the chemistry of graphene, Physical Chemistry Chemical Physics.17 28484–28504

Wang XY, Narita A, Müllen K (2018). Precision synthesis versus bulk-scale fabrication of graphenes. Nature Reviews Chemistry, 2(1), 0100.

Wang Z, Liu J, Wang W, Chen H, Liu Z, Yu Q, Zeng H, Sun L (2013). Aqueous phase preparation of graphene with low defect density and adjustable layers. Chemical Communications, 49(92), 10835–10837.

Wojtoniszak M, Chen X, Kalenczuk RJ, Wajda A, Lapczuk J, Kurzewski M, Drozdzik M, Chu PK, Borowiak-Palen E (2012). Synthesis, dispersion, and cytocompatibility of graphene oxide and reduced graphene oxide. Colloids and Surfaces B, vol. 89, pp. 79–85.

Xing R, Li Y, Yu HP (2016). Reparation of fluoro-functionalized graphene oxide via the Hunsdiecker reaction Chemical Communications. 52, 390–393

Yang ST, Chang Y, Wang H, Liu G, Chen S, Wang Y, Liu Y, Cao A (2010). Folding/aggregation of graphene oxide and its application in Cu2+ removal. J. Colloid Interface Sci. 351, 122–127. [CrossRef]

Yu H, Zhang B, Bulin C, Li R, Xing R (2016). High-efficient Synthesis of Graphene Oxide Based on Improved Hummers Method. Scientific Reports, 6.

Yumura T, Yamasaki A (2014). Roles of water molecules in trapping carbon dioxide molecules inside the interlayer space of graphene oxides. Phys. Chem. Chem. Phys. 16, 9656–9666. [CrossRef]

Zaaba NI, Foo KL, Hashim U, Tan SJ, Liu WW, Voon CH (2017). Synthesis of Graphene Oxide using Modified Hummers Method: Solvent Influence. Procedia Engineering, 184, 469–477.

Zhao G, Li J, Ren X, Chen C, Wang X (2011). Few-layered graphene oxide nanosheets as superior sorbents for heavy metal ion pollution management. Environ. Sci. Technol. 45, 10454–10462. [CrossRef]

Zhao J, Liu F, Wang Z, Cao X, Xing B (2015). Heteroaggregation of graphene oxide with minerals in aqueous phase. Environmental Science and Technology, 49(5), 2849–2857.

Zhou X, Huang W, Shi J, Zhao Z, Xia Q, Li Y,Wang H, Li Z (2014).A novel MOF/graphene oxide composite GrO@ MIL-101 with high adsorption capacity for acetone. J. Mater. Chem. A, 2, 4722–4730. [CrossRef]